J. Fluid Mech. (1991), *vol.* 229, *pp.* 365–388
Printed in Great Britain

Non-isothermal spreading of liquid drops on horizontal plates

By PETER EHRHARD[1] AND STEPHEN H. DAVIS[2]

[1] Institut für Reaktorbauelemente, Kernforschungszentrum Karlsruhe GmbH Postfach 3640, D-7500 Karlsruhe 1, Germany

[2] Department of Engineering Sciences and Applied Mathematics, McCormick School of Engineering and Applied Science, Northwestern University, Evanston, IL 60208, USA

(Received 16 March 1990 and in revised form 10 January 1991)

A viscous-liquid drop spreads on a smooth horizontal surface, which is uniformly heated or cooled. Lubrication theory is used to study thin drops subject to capillary, thermocapillary and gravity forces, and a variety of contact-angle-versus-speed conditions. It is found for isothermal drops that gravity is very important at large times and determines the power law for unlimited spreading. Predictions compare well with the experimental data on isothermal spreading for both two-dimensional and axisymmetric configurations. It is found that heating (cooling) retards (augments) the spreading process by creating flows that counteract (reinforce) those associated with isothermal spreading. For zero advancing contact angle, heating will prevent the drop from spreading to infinity. Thus, the heat transfer serves as a sensitive control on the spreading.

1. Introduction

The spreading of a liquid on a smooth solid is a fundamental problem in fluid mechanics. It exemplifies the general problem of moving contact lines, which enters a host of applications such as coating technology, mould filling and the performance in Space of fuel tanks. It involves the modelling of the local mechanics near the contact lines whenever a continuum theory of the motion is envisaged. A spreading drop involves bulk, surface and line forces intrinsically coupled through a free-boundary problem. The configuration is shown in figure 1.

Body forces affect the drop in a classical sense; gravity will greatly promote the spreading if the hydrostatic head is appreciable.

Surface forces enter the description through the liquid/gas interface on which surface tension acts. Further, if the contact line moves, and the no-slip condition is applied on the solid/liquid interface, then, as shown by Dussan V. & Davis (1974) there is a force singularity at the contact line. The implication is that on a continuum level there is effective slip at the liquid/solid interface. This is also a surface effect.

At the contact line there is a contact-angle condition. In the two-dimensional case, say, the interface slope h_x at the contact line at $x = a$ must satisfy the compatibility condition $h_x(a, t) = -\tan\theta$, where θ is the contact angle and the interface is located at $z = h(x, t)$, as shown in figure 1. One must specify a constitutive law for θ, since it is here that the chemistry of the surfaces has an effect. If the interface moves with speed U, then one may specify $\theta = F(U)$; this determines the mobility of the contact line. Dussan V. (1979) discusses such models and the data that underlie them. The contact-angle condition gives a line effect in the model description.

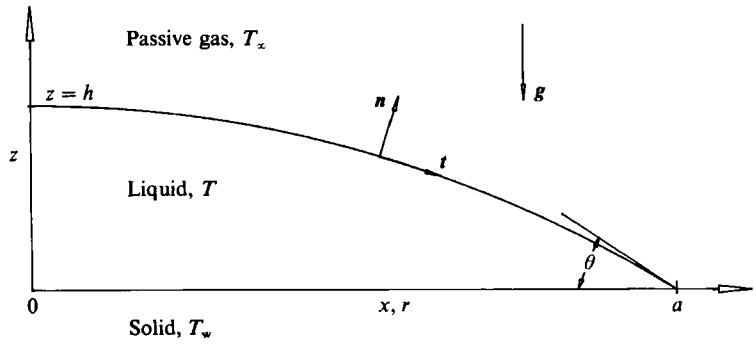

FIGURE 1. Sketch of the problem geometry.

There are a number of approaches to the modelling of the dynamics of spreading drops. These can be roughly categorized as (i) excision, (ii) microscopic and (iii) uniform analyses.

(i) Tanner (1979) considered viscous and capillary forces only and used lubrication theory to describe the bulk drop, away from the contact line. Analysis of the excised contact-line region is replaced by *a priori* statements about the 'outer' balances and about the drop shape. For unlimited spreading, he found power laws for the drop radius as a function of time t for large times. He found $a \sim t^{\frac{1}{7}}$ in two dimensions and $a \sim t^{\frac{1}{10}}$ in the axisymmetric case. Starov (1983), further, extracted the multiplicative prefactor in these forms. Lopez, Miller & Ruckenstein (1976) took a similar approach, but ignored capillarity, and instead included gravity or long-range molecular forces near $x = a$. They sought similarity solutions and found for the gravity-dominated drop that $a \sim t^{\frac{1}{5}}$ in two dimensions and $a \sim t^{\frac{1}{8}}$ in the axisymmetric case. They pointed out that these similarity solutions gave infinite shear stresses at the contact lines; the solutions thus break down at the main points of interest. The case in which long-range forces dominate leads to thin films with no discernible leading edges. See de Gennes (1985) for a review of these aspects. A *self-consistent* excision procedure with appropriate matching to a local wedge flow has been used extensively on contact-line problems by Dussan V.; see Ngan & Dussan V. (1989).

(ii) Another approach to spreading is that of de Gennes (1985) who wished to examine the small-scale physics of contact lines. He included in his model long-range van der Waals repulsions and so obtained a drop that possesses no contact line nearby, but instead found a thick drop that smoothly blends into a precursor film that extends from the main drop, sometimes far forward along the plate. On the one hand, there is no longer a contact line nearby to consider, and, on the other hand, he did not consider the actual contact line at the edge of the film. This approach may in fact lead to useful information on the functional form of F, but its direct pursuit requires one to examine thin films whose thicknesses are in the 10–100 Å range; these are essentially invisible to a continuum theory.

(iii) There is a uniform approach to the continuum theory in which one considers the whole drop including the contact line, inserts local slip nearby and poses $\theta = F(U)$. Greenspan (1978) posed such a model including both capillary and viscous forces and with F linear. He used lubrication theory for flat drops and obtained an evolutionary system giving the drop history.

The present paper aims to analyse the spreading of a viscous drop on a smooth, horizontal plate. The approach generalizes that of Greenspan (1978) in three ways. (i) The angle-versus-speed characteristic is generalized to $U = \kappa(\theta - \theta_A)^m$, where θ_A is

the (static) advancing contact angle and κ is an empirical coefficient. We term the factor m the mobility exponent. This form with $m = 1$ was used by Greenspan, while the case $m = 3$ is suggested for the apparent angle by Schwartz & Tejeda (1972), Hoffman (1975) and Tanner (1979) using data on contact-line dynamics. The case of constant contact angle, $m \to \infty$, has been considered by Hocking (1977, 1981, 1983), Hocking & Rivers (1982), Haley & Miksis (1991) and others. (ii) Gravity, acting vertically, is included. (iii) The plate is uniformly heated or cooled, compared to the surrounding gas. If the plate is hotter than the surrounding gas, then the non-isothermal liquid/gas interface will have the contact line hotter than the drop summit. Thermocapillarity will drive a flow in the viscous drop that will either augment or hinder the spreading. The heat transfer is conduction dominated in this lubrication limit.

The analysis obtains generalized evolution equations for the spreading in both two-dimensional and axisymmetric configurations. The equations are then examined in the limit of small capillary number in which spreading rates, interface shapes and velocity fields can be determined over the whole drop. A number of new results are obtained.

In the isothermal case solutions that include viscous forces, gravity and surface tension show how thin drops with negligible gravity effects can spread to such large size that gravity becomes important, as observed by Cazabat & Cohen Stuart (1986). When the static advancing angle $\theta_A = 0$, the drop spreads to infinity. The power laws obtained here agree very well with those of previous theory and experiment, validating both the lubrication theory and the choices of the mobility exponent $m = 3$.

In the non-isothermal case thermocapillary-driven flows create bulk flows that alter the spreading process. For example a drop with advancing contact angle $\theta_A = 0$ will spread forever under isothermal conditions. The same drop, if $\theta_A = 0$ still, will spread only finitely far if the plate is heated. If the plate is cooled, then a drop will spread further than otherwise. The heating or cooling can thus be used to control the spreading process.

2. Formulation

Consider a drop of liquid on a smooth, horizontal rigid plane located at a position $z = 0$ and kept at a constant temperature $T = T_W$. The drop is composed of a non-volatile Newtonian liquid with constant material properties and surrounded by a passive gas, whose viscosity and thermal conductivity are taken to be very small compared to those of the liquid; the far-field gas temperature is T_∞. The drop, shown in figure 1, is either two-dimensional in Cartesian coordinates (x, z) or axisymmetric in cylindrical coordinates (r, z). We shall examine both cases and denote equation numbers by p (plane) and a (axisymmetric), respectively. The shape of the interface between the spreading liquid and the ambient gas is denoted by $z = h$, and the position of the contact line is given by either $x = a$ or $r = a$.

The velocity and thermal fields in the liquid are governed by the Navier–Stokes, the continuity, and the energy equations:

$$\rho\left\{\frac{\partial \boldsymbol{v}}{\partial t} + \boldsymbol{v}\cdot\boldsymbol{\nabla}\boldsymbol{v}\right\} = -\boldsymbol{\nabla}p + \mu\nabla^2\boldsymbol{v} - \rho g\boldsymbol{k}, \tag{2.1}$$

$$\boldsymbol{\nabla}\cdot\boldsymbol{v} = 0, \tag{2.2}$$

$$\rho c_p \left\{ \frac{\partial T}{\partial t} + \boldsymbol{v} \cdot \boldsymbol{\nabla} T \right\} = \lambda \nabla^2 T. \tag{2.3}$$

where $\boldsymbol{k} = (0, 1)$, $\boldsymbol{v} = (u, w)$ is the velocity vector, p is the pressure and T is the temperature of the liquid. Here g is the magnitude of the gravitational acceleration, ρ is the density, μ is the viscosity, c_p is the specific heat, and λ the heat conductivity of the liquid.

Equations (2.1)–(2.3) are subject to the following boundary conditions at the liquid/solid interface:

$$z = 0: \quad u = \beta' \frac{\partial u}{\partial z}, \quad w = 0, \quad T = T_{\mathrm{W}}. \tag{2.4}$$

The rigid plane is considered to be impenetrable, perfectly conducting material. Following Dussan V. & Davis (1974), the no-slip condition at the rigid boundary is relaxed to avoid the appearance of a shear-stress singularity at the moving contact line. The slip coefficient β' in (2.4) is taken to be a small constant.

At the liquid/gas interface there are the following conditions:

$$z = h: \quad w - \frac{\partial h}{\partial t} = \frac{\partial h}{\partial x} u, \tag{2.5p}$$

$$w - \frac{\partial h}{\partial t} = \frac{\partial h}{\partial r} u, \tag{2.5a}$$

$$\boldsymbol{n} \cdot \boldsymbol{T} \cdot \boldsymbol{n} = 2H\sigma, \tag{2.6}$$

$$\boldsymbol{t} \cdot \boldsymbol{T} \cdot \boldsymbol{n} = \boldsymbol{t} \cdot \boldsymbol{\nabla} \sigma, \tag{2.7}$$

$$-\lambda \frac{\partial T}{\partial n} = \frac{\lambda_\infty}{\delta} (T - T_\infty). \tag{2.8}$$

Here $\boldsymbol{T}$ denotes the stress tensor of the liquid, $\boldsymbol{n}$ and $\boldsymbol{t}$ are the unit normal and tangential vectors with $\boldsymbol{n}$ pointing out of the liquid (see figure 1). Equation (2.5) is the kinematic condition while (2.6) and (2.7) give the dynamic conditions, balancing normally and tangentially, the stress components across the liquid/gas interface. The mean curvature H in (2.6) is given by

$$2H = \boldsymbol{\nabla} \cdot \{[1 + |\boldsymbol{\nabla} h|^2]^{-\frac{1}{2}} \boldsymbol{\nabla} h\}. \tag{2.9}$$

Here the surface tension σ depends linearly on temperature

$$\sigma(T) = \sigma_{\mathrm{W}} - \gamma(T - T_{\mathrm{W}}), \tag{2.10}$$

$\gamma > 0$, so that (2.7) incorporates the effects of thermocapillarity. The surface tension in (2.10) is denoted by σ and σ_{W} is the surface tension at a temperature T_{W}.

The thermal boundary condition at the liquid/gas interface is chosen to be of third type, i.e. we use a mixed condition on the heat flux and the local temperature, involving the parameter group $\lambda_\infty / \lambda\delta$, which contains all limiting cases between an adiabatic and a perfectly conducting boundary. Here λ_∞ denotes the thermal conductivity of the ambient gas, while δ is the thickness of the thermal boundary layer established within the gas. Such a model may break down near the contact line when h is smaller than δ but such a model is a reasonable one for an initial investigation.

We must specify initial conditions, symmetry or smoothness conditions, and volume constraints on the drop shape. These are as follows:

$$h(x,0) = h_0(x), \quad h_0(a_0) = 0, \quad a(0) = a_0, \tag{2.11p}$$

$$h(r,0) = h_0(r), \quad h_0(a_0) = 0, \quad a(0) = a_0, \tag{2.11a}$$

$$\frac{\partial h_0}{\partial x}(0) = 0, \quad \frac{\partial^3 h_0}{\partial x^3}(0) = 0, \tag{2.12p}$$

$$\frac{\partial h_0}{\partial r}(0) = 0, \quad \lim_{r\to 0}\left\{r\frac{\partial^3 h_0}{\partial r^3}(r)\right\} = 0, \tag{2.12a}$$

$$\frac{\partial h_0}{\partial x}(a_0) = -\tan\theta_0, \tag{2.13p}$$

$$\frac{\partial h_0}{\partial r}(a_0) = -\tan\theta_0. \tag{2.13a}$$

Thus, the drop is symmetric and smooth initially with an edge at a_0 and an initial contact angle of θ_0. The volume of the drop is conserved during the spreading process and can be calculated from the initial drop shape. The volume per unit width in the two-dimensional case is given by

$$V_0 = \int_{-a_0}^{a_0} h_0(x)\,\mathrm{d}x, \tag{2.14p}$$

while the volume in the axisymmetric case is given by

$$V_0 = 2\pi\int_0^{a_0} r h_0(r)\,\mathrm{d}r. \tag{2.14a}$$

For $t > 0$ the drop retains its symmetries; the edge, symmetry, smoothness and volume conditions are thus given as follows:

$$h[a(t),t] = 0 \quad \text{(condition of contact)}, \tag{2.15}$$

$$\left.\begin{aligned} &\frac{\partial h}{\partial x}(0,t) = 0, \quad \frac{\partial^3 h}{\partial x^3}(0,t) = 0 && (2.16p)\\ &\frac{\partial h}{\partial r}(0,t) = 0, \quad \lim_{r\to 0}\left\{r\frac{\partial^3 h}{\partial r^3}(0,t)\right\} = 0 && (2.16a)\end{aligned}\right\} \text{(symmetry and smoothness conditions)},$$

$$\left.\begin{aligned} &\frac{\partial h}{\partial x}[a(t),t] = -\tan\theta(t) && (2.17p)\\ &\frac{\partial h}{\partial r}[a(t),t] = -\tan\theta(t). && (2.17a)\end{aligned}\right\} \text{(contact-angle condition)},$$

$$\left.\begin{aligned} &\int_{-a(t)}^{a(t)} h(x,t)\,\mathrm{d}x = V_0 && (2.18p)\\ &2\pi\int_0^{a(t)} r h(r,t)\,\mathrm{d}r = V_0 && (2.18a)\end{aligned}\right\} \text{(conservation of volume)}.$$

Based on various experimental results, Dussan V. (1979) discusses how the apparent contact angle depends on the speed, $\partial a/\partial t$, of the contact line. In the

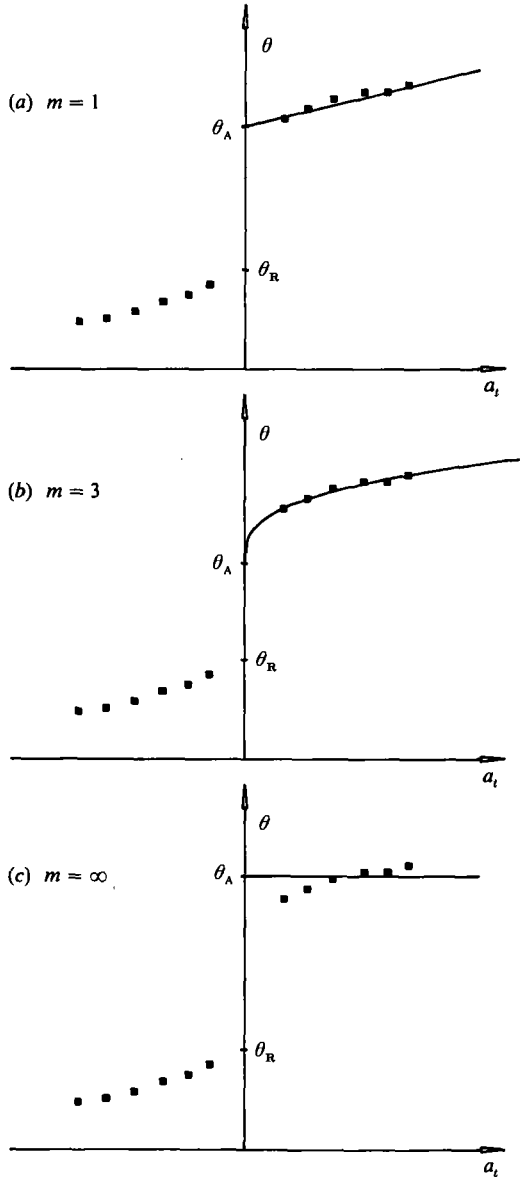

FIGURE 2. Typical measurements of contact angle after Dussan V. (1979); symbols represent experimental data, solid lines correspond to various mobility exponents m in model equation (2.19).

following we take the angle θ to be given by a similar form; the constitutive form is chosen here to be

$$a_t = \kappa(\theta - \theta_A)^m, \quad m \geqslant 1, \tag{2.19}$$

where $\kappa > 0$ is an empirical constant and $\theta_A \geqslant 0$ is the (static) advancing contact angle. The typical behaviour of experimental data (from Dussan V. 1979) and the above model (2.19) for various m are shown in figure 2. The form (2.19) for $m = 3$ is suggested by the data of Schwartz & Tejeda (1972), Hoffman (1975), and Tanner (1979).

3. Scaling and the lubrication approximation

The analysis of Greenspan (1978) uses lubrication theory to simplify the governing system for isothermal spreading. The present work generalizes that of Greenspan in three ways. (i) The effects of gravity are included. (ii) The contact-angle-versus-speed characteristic (2.19) allows for power-law behaviour with exponent m; Greenspan used $m = 1$. (iii) Non-isothermal spreading is allowed through the action of thermocapillarity.

We generalize the analysis of Greenspan (1978) by introducing the following set of dimensionless variables:

$$\left.\begin{aligned} x^* &= \frac{x}{a_0}, \quad r^* = \frac{r}{a_0}, \quad z^* = \frac{z}{a_0\theta_0}, \quad t^* = \frac{\kappa\theta_0^m}{a_0}t, \\ u^* &= \frac{u}{\kappa\theta_0^m}, \quad w^* = \frac{w}{\kappa\theta_0^{1+m}}, \quad p^* = \frac{a_0\theta_0^{2-m}}{\mu\kappa}p, \\ T^* &= \frac{T-T_\infty}{T_W-T_\infty}, \quad \Theta^* = \frac{\theta}{\theta_0}, \quad V^* = \frac{V}{V_0}. \end{aligned}\right\} \tag{3.1}$$

Thus, the space variables (x, z) or (r, z) are scaled using the initial shape of the drop in the horizontal and vertical directions, respectively. The timescale is constructed using the horizontal lengthscale a_0 together with an estimate of the initial speed of the contact line, $\kappa\theta_0^m$, which is obtained by use of (2.19) for $\theta_A = 0$. Conservation of mass determines the velocity scales. The pressure scale is obtained by balancing the pressure gradients and viscous terms in the horizontal component of the Navier–Stokes equations. The temperature scaling is chosen to allow the largest possible (unit order) temperature difference.

If scalings (3.1) are introduced into system (2.1)–(2.19), the leading-order asymptotic equations valid as $\theta_0 \to 0$ lead to the 'lubrication approximation':

$$-p_x + u_{zz} = 0, \tag{3.2p}$$

$$-p_r + u_{zz} = 0, \tag{3.2a}$$

$$-p_z - \frac{G}{C} = 0, \tag{3.3}$$

$$u_x + w_z = 0, \tag{3.4p}$$

$$(ru)_r + rw_z = 0, \tag{3.4a}$$

$$T_{zz} = 0, \tag{3.5}$$

where subscripts denote partial differentiation. For simplicity, all asterisks have been dropped. The boundary conditions are as follows:

$$z = 0: \quad u = \beta u_z, \quad w = 0, \quad T = 1; \tag{3.6}$$

$$z = h: \quad w - h_t = uh_x, \tag{3.7p}$$

$$w - h_t = uh_r, \tag{3.7a}$$

$$-Cp = h_{xx}, \tag{3.8p}$$

$$-Cp = h_{rr} + \frac{1}{r}h_r, \tag{3.8a}$$

$$\Delta C u_z = -(T_x + h_x T_z), \tag{3.9p}$$

$$\Delta C u_z = -(T_r + h_r T_z), \tag{3.9a}$$

$$T_z + BT = 0. \tag{3.10}$$

Further, for $t = 0$

$$h(x,0) = h_0(x), \quad h_0(1) = 0, \quad a(0) = 1, \tag{3.11p}$$

$$h(r,0) = h_0(r), \quad h_0(1) = 0, \quad a(0) = 1, \tag{3.11a}$$

$$h_{0x}(0) = 0, \quad h_{0xxx}(0) = 0, \tag{3.12p}$$

$$h_{0r}(0) = 0, \quad \lim_{r\to 0}[rh_{0rrr}(r)] = 0, \tag{3.12a}$$

$$h_{0x}(1) = -1, \tag{3.13p}$$

$$h_{0r}(1) = -1, \tag{3.13a}$$

$$1 = \int_{-1}^{1} h_0(x)\,\mathrm{d}x, \tag{3.14p}$$

$$1 = 2\pi \int_0^1 r h_0(r)\,\mathrm{d}r, \tag{3.14a}$$

and, for $t > 0$

$$h(a,t) = 0, \tag{3.15}$$

$$h_x(0,t) = 0, \quad h_{xxx}(0,t) = 0, \tag{3.16p}$$

$$h_r(0,t) = 0, \quad \lim_{r\to 0}[rh_{rrr}(r,t)] = 0, \tag{3.16a}$$

$$h_x(a,t) = -\Theta(t), \tag{3.17p}$$

$$h_r(a,t) = -\Theta(t), \tag{3.17a}$$

$$1 = \int_{-a(t)}^{a(t)} h(x,t)\,\mathrm{d}x, \tag{3.18p}$$

$$1 = 2\pi \int_0^{a(t)} r h(r,t)\,\mathrm{d}r. \tag{3.18a}$$

The instantaneous contact angle $\Theta(t)$ is expressed in terms of the speed of the contact line, i.e.

$$\Theta(t) = [a_t(t)]^{1/m} + \Theta_A. \tag{3.19}$$

A number of dimensionless parameters arise. These are the capillary number C, the Bond number G, the thermocapillary number ΔC, the Biot number B, as well as the slip coefficient β. The definitions are as follows:

$$\left.\begin{aligned} C &= \frac{\mu\kappa}{\sigma_W \theta_0^{3-m}}, \quad G = \frac{\rho g a_0^2}{\sigma_W}, \quad B = \frac{\lambda_\infty a_0 \theta_0}{\lambda\delta}, \\ \Delta C &= \frac{\mu\kappa}{\gamma(T_W - T_\infty)\,\theta_0^{1-m}}, \quad \beta = \frac{\beta'}{a_0\theta_0}. \end{aligned}\right\} \tag{3.20}$$

The capillary number compares the dissipative effects of angle-versus-speed variations to mean surface tension. The Bond number relates gravity forces to mean

surface tension. The thermocapillary number measures the fractional thermal change in the surface tension. Finally, the Biot number characterizes the quality of the heat transfer occurring at the liquid/gas interface. In particular $B \to 0$ and $B \to \infty$ give the adiabatic and the perfectly conducting limits, respectively.

The simplified Navier–Stokes equations (3.2) and (3.3) show that the horizontal pressure gradient is balanced by the viscous shear stresses, while vertically there is a hydrostatic balance. From the energy equation (3.5) we see that heat is transported across the drop mainly by conduction.

4. Derivation of the evolution equation

Within the lubrication approximation the Navier–Stokes equations (3.2) and (3.3) and the continuity equation (3.4), decouple from the heat transport. Therefore, one can solve for the thermal field, governed by (3.5) and subject to the thermal boundary conditions in (3.6) and (3.10) to obtain

$$T = \frac{1+B(h-z)}{1+Bh}. \tag{4.1}$$

The position of the liquid/gas interface, $h(x,t)$ or $h(r,t)$ is unknown *a priori*, and through h the temperature will depend on both space coordinates as well as on time. The interface temperature can be found from (4.1) as

$$T(h) = \frac{1}{1+Bh}. \tag{4.2}$$

Equation (4.2) shows for both the adiabatic and the perfectly conducting limits that the temperature along the liquid/gas interface is constant. In fact,

$$\left.\begin{aligned} B \to 0: &\quad T(h) = 1, \\ B \to \infty: &\quad T(h) = 0. \end{aligned}\right\} \tag{4.3}$$

The adiabatic limit results in the interface temperature T_w, while the perfectly conducting limit gives T_∞. In order to have variations in temperature and therefore surface-tension gradients along the interface, we can only have the Biot number in the range $0 < B < \infty$.

We use continuity equation (3.4) and integrate across the liquid layer, using the appropriate boundary conditions in (3.6) and (3.7) to obtain

$$h_t + \frac{\partial}{\partial x}\int_0^h u\,\mathrm{d}z = 0, \tag{4.4p}$$

$$h_t + \frac{\partial}{\partial r}\int_0^h u\,\mathrm{d}z = 0. \tag{4.4a}$$

The integration of the momentum equation (3.3) and application of the normal-stress boundary condition (3.8) gives

$$h_{xx} + Cp(x,0,t) - Gh = 0, \tag{4.5p}$$

$$h_{rr} + \frac{1}{r}h_r + Cp(r,0,t) - Gh = 0. \tag{4.5a}$$

The horizontal momentum equation (3.2) is integrated twice with respect to z and the boundary conditions in (3.6) and (3.9) are applied, to obtain

$$C\int_0^h u\,\mathrm{d}z = \left\{\frac{h^3}{3}+\beta h^2\right\}\mathrm{D}_{3x}h+\frac{C}{\Delta C}\frac{B}{(1+Bh)^2}\left\{\frac{h^2}{2}+\beta h\right\}h_x, \tag{4.6p}$$

$$C\frac{1}{r}\int_0^h (ru)\,\mathrm{d}z = \left\{\frac{h^3}{3}+\beta h^2\right\}\mathrm{D}_{3r}h+\frac{C}{\Delta C}\frac{B}{(1+Bh)^2}\left\{\frac{h^2}{2}+\beta h\right\}h_r, \tag{4.2a}$$

Here the operators D_{3x} and D_{3r} are defined as

$$\mathrm{D}_{3x}h = \{h_{xx}-Gh\}_x, \tag{4.7p}$$

$$\mathrm{D}_{3r}h = \left\{h_{rr}+\frac{1}{r}h_r-Gh\right\}_r. \tag{4.7a}$$

Equations (4.4) and (4.6) then provide an evolution equation for the drop shape as follows:

$$Ch_t+\left\{\left[\frac{h^3}{3}+\beta h^2\right]\mathrm{D}_{3x}h+\frac{C}{\Delta C}\frac{B}{(1+Bh)^2}\left[\frac{h^2}{2}+\beta h\right]h_x\right\}_x = 0. \tag{4.8p}$$

$$Ch_t+\frac{1}{r}\left\{\left[\frac{h^3}{3}+\beta h^2\right]r\,\mathrm{D}_{3r}h+\frac{C}{\Delta C}\frac{B}{(1+Bh)^2}\left[\frac{h^2}{2}+\beta h\right]rh_r\right\}_r = 0. \tag{4.8a}$$

The evolution equation (4.8) allows us to bypass the free-boundary problem for h, though the edge position $a(t)$ is still unknown. The edge, symmetry and volume condition on the drop shape, (3.11)–(3.19), still apply.

In what follows, the Biot number will be considered to be much smaller than unity,

$$B \ll 1, \tag{4.9}$$

so that the effect of thermocapillarity, as shown in evolution equations (4.8), is incorporated only in the product $CB/\Delta C$. This serves as the effective Marangoni number $\hat{M}$.

$$\hat{M} = \frac{CB}{\Delta C}. \tag{4.10}$$

When $\hat{M} > 0$, the plate is heated with respect to the gas, while if $\hat{M} < 0$, it is cooled.

4.1. *The flow field*

After the solutions of the evolution equation (4.8) are known, one can calculate the velocity field:

$$\left.\begin{aligned} Cu &= [h(z+\beta)-\tfrac{1}{2}z^2]\,\mathrm{D}_{3x}h+\hat{M}h_x(z+\beta),\\ Cw &= [\tfrac{1}{6}z^3-\tfrac{1}{2}z^2-\beta hz]\,\mathrm{D}_{4x}h-[\tfrac{1}{2}z^2+\beta z]\,h_x\,\mathrm{D}_{3x}h-\hat{M}[\tfrac{1}{2}z^2+\beta z]\,h_{xx}, \end{aligned}\right\} \tag{4.11p}$$

$$\left.\begin{aligned} Cu &= [h(z+\beta)-\tfrac{1}{2}z^2]\,\mathrm{D}_{3r}h+\hat{M}h_r(z+\beta),\\ Cw &= [\tfrac{1}{6}z^3-\tfrac{1}{2}z^2h-\beta hz]\,\mathrm{D}_{4r}h-[\tfrac{1}{2}z^2+\beta z]\,h_r\,\mathrm{D}_{3r}h-\hat{M}\,[\tfrac{1}{2}z^2+\beta z]\frac{1}{r}(rh_r)_r \end{aligned}\right\} \tag{4.11a}$$

where the operators D_{4x} and D_{4r} are defined by

$$D_{4x} h = \frac{\partial}{\partial x}(D_{3h} h), \tag{4.12p}$$

$$D_{4r} h = \frac{1}{r}\frac{\partial}{\partial r}[r(D_{3r} h)]. \tag{4.12a}$$

5. The $C \to 0$ problem

The evolutionary system (4.8) and (3.11)–(3.19) was derived for all parameters (3.20) of unit order, in particular $C = O(1)$ and $\beta = O(1)$. There are two secondary limits that are of interest.

The limit $C \to \infty$ can be extracted from the general one by defining a new timescale τ,

$$\tau = C^{-1} t. \tag{5.1}$$

By this transformation the evolution equation (4.8) becomes free of C, while the limit $C \to \infty$ removes the time derivative from the edge condition (3.17) and (3.19). We see that limiting form becomes $\Theta = \Theta_A$, the fixed contact-angle condition used extensively by Hocking (1977, 1981, 1983). Given $C \to \infty$, he examines the small-β limit and finds that the natural parameter that emerges is ϵ,

$$\epsilon = \frac{1}{|\ln \beta|} \ll 1. \tag{5.2}$$

In our terms Hocking examines the regime

$$C^{-1} \ll \epsilon. \tag{5.3}$$

Equation (2.19) gives that $C \propto \kappa$, so that large κ means that the contact line is very mobile. As κ^{-1} increases, the motion is retarded; the slope of the a_t versus Θ characteristic of figure 2 measures contact-line *dissipation*, as shown by Davis (1980).

The limit $C \to 0$ was proposed by Greenspan (1978). Small C implies that the contact line is not very mobile. This regime is given by

$$C \ll \epsilon, \tag{5.4}$$

which is governed by the general system by setting the time derivative in the evolution equation to zero; the spreading is then quasi-steady.

Given the definition (3.20) of C and Hocking's results, the first model limits spreading by slippage, while the second model limits the spreading by contact-line mobility.

In this paper only the quasi-steady limit, $C \to 0$, will be analysed. As discussed by Rosenblat & Davis (1985), the dropping of the unsteady term in (4.8) leads to an 'outer' solution in time. The initial condition on h must be dropped while that on $a(t)$ is enforced. The unsteady term a_t in the contact-line conditions (3.17) and (3.19), is, of course, retained since this allows the drop to evolve. Details of the analysis are shown for the two-dimensional drop. The details are similar for the axisymmetric drop and only results are given.

Equation (4.8) with $B \ll 1$ and $C \to 0$ can be integrated once; the integration constant is zero owing to the symmetry conditions. Our numerical integrations of the

resulting equation show that the solutions are indistinguishable for cases when the slip coefficient $\beta = 10^{-6}$ and $\beta = 0$. This is consistent with Greenspan's (1978) observation (for the case $G = 0$, $m = 1$, $\hat{M} = 0$) that the imposition of slip is not necessary if one examines *only* the leading term of the small-C approximation.

If β is set to zero and the Biot number is small, then the once-integrated evolution equation becomes

$$(h_{xx} - Gh)_x + \tfrac{3}{2}\hat{M}\frac{h_x}{h} = 0. \tag{5.5p}$$

Similarly,

$$\left[\frac{1}{r}(rh_r)_r - Gh\right]_r + \tfrac{3}{2}\hat{M}\frac{h_r}{h} = 0. \tag{5.5a}$$

6. Results: isothermal spreading

When the system is isothermal, $\hat{M} = 0$, (5.5) can be solved, subject to the conditions of symmetry (3.16), of contact (3.15) and of constant volume (3.18). The results (Hocking 1983) are

$$h(x,t) = \tfrac{1}{2}G^{\frac{1}{3}}\frac{\cosh xG^{\frac{1}{3}} - \cosh aG^{\frac{1}{3}}}{\sinh aG^{\frac{1}{3}} - aG^{\frac{1}{3}}\cosh aG^{\frac{1}{3}}}, \tag{6.1p}$$

and

$$h(r,t) = \frac{G^{\frac{1}{3}}}{a}\frac{I_0(rG^{\frac{1}{3}}) - I_0(aG^{\frac{1}{3}})}{I_1(aG^{\frac{1}{3}}) - \frac{1}{2}aG^{\frac{1}{3}}I_0(aG^{\frac{1}{3}})}, \tag{6.1a}$$

where I_n is the modified Bessel function of the first kind.

Forms (6.1) are now substituted into the contact-angle conditions (3.17) and (3.19) to yield

$$a_t^{1/m} + \Theta_A = -h_x(a,t) = \tfrac{1}{2}G[aG^{\frac{1}{3}}\coth aG^{\frac{1}{3}} - 1]^{-1}, \tag{6.2p}$$

$$a_t^{1/m} + \Theta_A = -h_r(a,t) = \frac{G}{2\pi a}\frac{I_1(aG^{\frac{1}{3}})/I_0(aG^{\frac{1}{3}})}{\frac{1}{2}aG^{\frac{1}{3}} - I_1(aG^{\frac{1}{3}})/I_0(aG^{\frac{1}{3}})}. \tag{6.2a}$$

Equations (6.2) are differential equations for $a = a(t)$ subject to the initial condition $a(0) = 1$.

Case 1: $\Theta_A > 0$, $G = 0$

The drop spreads to an equilibrium configuration. This is governed by (6.2p) with $a_t = 0$, $a = a_\infty$, and h_x replaced by its $G = 0$ limit. The result is

$$a_\infty^0 = \left(\frac{3}{2\Theta_A}\right)^{\frac{1}{3}} \tag{6.3p}$$

$$a_\infty^0 = \left(\frac{4}{\pi\Theta_A}\right)^{\frac{1}{3}}. \tag{6.3a}$$

Clearly, given the volume of the drop, the smaller the contact angle, the larger the final size. This final state is independent of exponent m. One can easily show also by perturbing (6.2) about the final state (6.3) that there is exponential approach to equilibrium. This is always the case for limited spreading, the spreading to $a = a_\infty < \infty$.

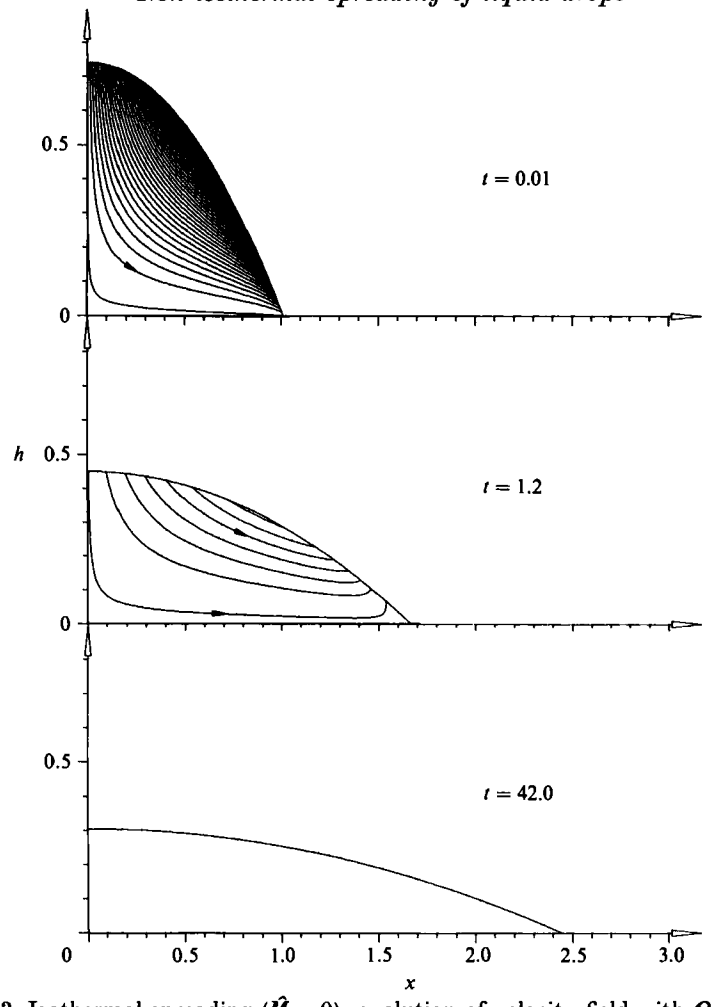

FIGURE 3. Isothermal spreading ($\hat{M} = 0$): evolution of velocity field with $\Theta_A = 0.25$, and $G = 0.05$. Instantaneous streamlines are given in steps $\Delta\psi = 0.01$.

Case 2: $\Theta_A > 0$, $G > 0$

Gravity acting vertically downward will flatten the drop centre, accelerate the spreading, and increase a_∞. In fact, for small G,

$$a_\infty \sim a_\infty^0 (1 + \tfrac{1}{30} a_\infty^{02} G) \tag{6.4p}$$

and

$$a_\infty \sim a_\infty^0 (1 + \tfrac{1}{72} a_\infty^{02} G), \tag{6.4a}$$

and a_∞^0 is given by (6.3).

Figure 3 shows the velocity fields in the approach to steady state where the density of the streamlines indicates the speed. Notice that the fluid is flowing downward, from the summit towards the contact line, and particularly downward along the liquid/gas interface.

Case 3: $\Theta_A = 0$, $G = 0$

Since $\Theta_A = 0$, the drop will experience unlimited spreading, i.e. $a \to \infty$ as $t \to \infty$. When $G = 0$, (6.2p) has the form

$$a^2 a_t^{1/m} = \tfrac{3}{2}. \tag{6.5p}$$

Reference	Plane $a \propto t^n$ n	Axisymmetric $a \propto t^n$ n	Dominant force
Experiments			
Tanner (1979)	0.148	0.106–0.112	ST
Cazabat & Cohen Stuart (1986)	—	$\frac{1}{10}$*	ST
	—	$\frac{1}{8}$*	G
Chen (1988)	—	0.080–0.135	ST
Theory			
Lopez *et al.* (1976)	$\frac{1}{5}$	$\frac{1}{8}$	G
Tanner (1979)	$\frac{1}{7}$	$\frac{1}{10}$	ST
Starov (1983)	—	$\frac{1}{10}$	ST
Greenspan (1978) $m = 1$	$\frac{1}{3}$	$\frac{1}{4}$	ST
Present results $m = 1$	$\frac{1}{3}$	$\frac{1}{4}$	ST
	$\frac{1}{2}$	$\frac{1}{3}$	G
Present results $m = 3$	$\frac{1}{7}$	$\frac{1}{10}$	ST
	$\frac{1}{4}$	$\frac{1}{7}$	G

TABLE 1. Isothermal spreading results. The symbols ST and G denote surface-tension and gravity dominance, respectively. The asterisk indicates that error bars were not given.

Hence, as $t \to \infty$,

$$a \sim c_m t^{1/(2m+1)}, \tag{6.6p}$$

where

$$c_m = [(2m+1)(\tfrac{3}{2})^m]^{1/(2m+1)}. \tag{6.7p}$$

Similarly, in the axisymmetric case

$$a^3 a_t^{1/m} = 8, \tag{6.5a}$$

and for $t \to \infty$

$$a \sim c_m t^{1/(3m+1)}, \tag{6.6a}$$

where

$$c_m = [(3m+1)\,8^m]^{1/(3m+1)}. \tag{6.7a}$$

For the exponent $m = 1$, formulae (6.6p) and (6.6a) give $a \sim t^{\frac{1}{3}}$ and $a \sim t^{\frac{1}{4}}$, respectively. As shown in table 1, this behaviour is that of Greenspan (1978). For the exponent $m = 3$, these formulae give $a \sim t^{\frac{1}{7}}$ and $a \sim t^{\frac{1}{10}}$. The former agrees with the excision result of Tanner (1979) and agrees with his experiment. The latter agrees with the excision result of Tanner (1979) and Starov (1983) and the experiments of Tanner (1979), Cazabat & Cohen Stuart (1986) and Chen (1988). The exponent in form (6.6a) has been inferred by de Gennes (1985) by presuming a spherical cap for h and assuming a form (2.19) for the contact angle. He selects the value $m = 3$ by consideration of van der Waals attractions in a precursor film.

The present results in both geometries support the use of the present uniform theory and the mobility exponent $m = 3$, for capillary-dominated spreading.

Case 4: $\Theta_A = 0$, $G > 0$

Since $\Theta_A = 0$, the drop will experience unlimited spreading in that $a \to \infty$ as $t \to \infty$. If one inspects (6.2), one sees that gravity should have a profound effect on the spreading process. In case 3, $h_x(a, t)$ was approximated for small G with fixed a. However, when the spreading is unlimited, any fixed value of G, no matter how small will eventually result in $aG^{\frac{1}{3}}$ becoming large; the limits $a \to \infty$, $G \to 0$ and $G \to 0$, $a \to \infty$ are not equivalent.

When $aG^{\frac{1}{3}}$ is large, (6.2p) becomes

$$a a_t^{1/m} = \tfrac{1}{2} G^{\frac{1}{3}}, \tag{6.8p}$$

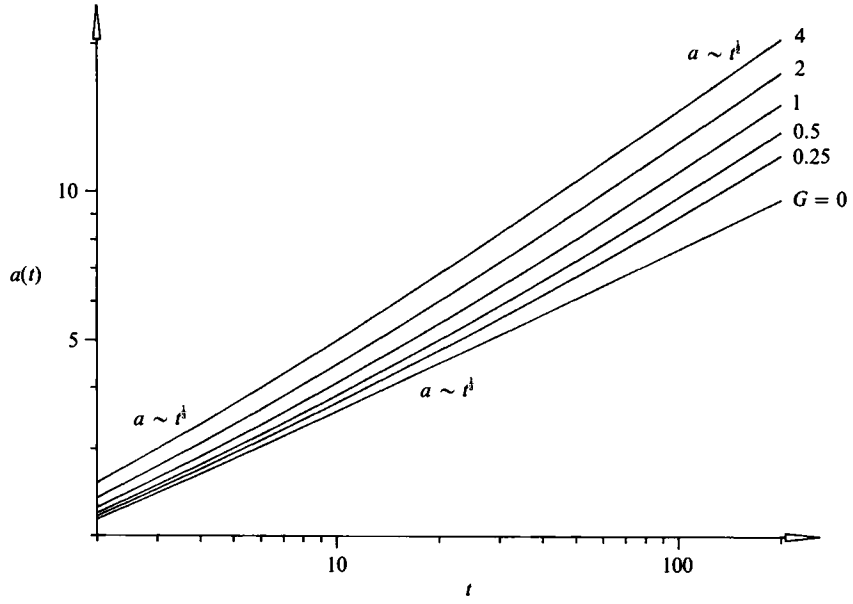

FIGURE 4. Isothermal spreading ($\hat{M} = 0$): positions of contact lines as function of time for various G with $\Theta_A = 0$.

so that as $t \to \infty$
$$a \sim d_m t^{1/(m+1)}, \tag{6.9p}$$

where
$$d_m = [(\tfrac{1}{2}G^{\frac{1}{3}})^m (m+1)]^{1/(m+1)}. \tag{6.10p}$$

Similarly, in the axisymmetric case, (6.2a) gives
$$a^2 a_t^{1/m} = 2G^{\frac{1}{3}}, \tag{6.8a}$$

so that as $t \to \infty$,
$$a \sim d_m t^{1/(2m+1)}, \tag{6.9a}$$

where
$$d_m = [2G^{\frac{1}{3}}(2m+1)]^{1/(2m+1)}. \tag{6.10a}$$

For the exponent $m = 1$, formulae (6.9p) and (6.9a) give $a \sim t^{\frac{1}{3}}$ and $a \sim t^{\frac{1}{5}}$, respectively. These results are new. For the exponent $m = 3$, these formulae give $a \sim t^{\frac{1}{4}}$ and $a \sim t^{\frac{1}{7}}$, respectively. Both of these differ slightly from the excision results of Lopez *et al.* (1976). The axisymmetric-spreading data of Cazabat & Cohen Stuart (1986) seem to agree better with the form $t^{\frac{1}{5}}$ than our $t^{\frac{1}{7}}$, suggesting that the mobility exponent $m = 3.5$ might give a better fit for their data.

The present results in both geometries support the use of the present uniform theory with a mobility exponent m equal to somewhat greater than 3.

The results show that the long-time spreading with gravity is substantially accelerated compared to the case $G = 0$, given the same mobility exponent m. The fact that gravity promotes spreading is no surprise. What seems paradoxical is the fact that a thin drop, which at early times is negligibly affected by gravity, will be greatly affected by gravity later when it is much thinner. This is consistent with Cazabat & Cohen Stuart (1986) who have conducted spreading experiments on smooth surfaces with axisymmetric drops under isothermal conditions. They report two different scaling laws during the spreading, depending on whether or not gravity is important. In a first phase of the spreading process they found capillary effects to be dominant while, in a second phase, for larger t, the influence of gravity seems to be controlling the process. This behaviour can be understood as follows. At early

times the hydrostatic pressures are small compared to capillary forces, but as the drop becomes flatter and flatter, the curvature goes to zero faster than the thickness and the small hydrostatic pressures ultimately dominate.

Figure 4 illustrates this behaviour; it shows our numerical solution of (6.2p) for $m = 1$ and various G. Note that as $t \to \infty$, the drop width $a \sim t^{\frac{1}{5}}$ when $G \neq 0$; compare this to the $G = 0$ result, $a \sim t^{\frac{1}{3}}$. Note as well that if one excludes initial transients, that the $G = 0$ behaviour $a \sim t^{\frac{1}{3}}$ is valid for early times even if $G \neq 0$. These results are consistent with the observations of Cazabat & Cohen Stuart (1986). They find that in practice the two ranges are not separated by values of the instantaneous Bond number $G^{(a)}$,

$$G^{(a)} = \frac{\rho g a^2(t)}{\sigma}, \tag{6.11}$$

viz. $G^{(a)} < 1$ meaning capillary domination and $G^{(a)} > 1$ meaning gravity domination. They are demarcated by fixed values of $a^{-\frac{3}{2}} a_t$.

7. Results: non-isothermal spreading

When the plate is heated or cooled, there are thermocapillary forces that render the drop dynamic; fluid flow is always present. The shape of the drop for small Biot number is governed for $C \to 0$ by (5.5). When this is integrated once, we find for the plane geometry that

$$h_{xx} - Gh + \tfrac{3}{2}\hat{M} \ln h = -s_1 \tag{7.1p}$$

where s_1 is a constant. Clearly, both h and h_x are regular at $x = a$ while the curvature undergoes rapid variations.

Similarly, in the axisymmetric case

$$\frac{1}{r}(rh_r)_r - Gh + \tfrac{3}{2}\hat{M} \ln h = -s_1. \tag{7.1a}$$

The curvature singularity at the contact lines implied by (7.1) is present even when the drop has spread to its final shape. Its presence is a result of flow against a 'static' contact line across which there is a change in boundary data from prescribed velocity to prescribed shear stress. It results in logarithmically infinite pressures but finite forces, e.g. see Dussan V. (1987, equation 4.19). Such weak singularities occur in a variety of situations such as at the lip in die swell, e.g. see Davis (1980) for a review.

In all that follows, the Marangoni number $\hat{M}$ is non-zero giving thermocapillary-driven motions in the drop. For reason of clarity we neglect gravitational effects ($G = 0$). For small values of $|\hat{M}|$, perturbation theory can be used to solve (7.1), subject to the symmetry (3.16) and contact conditions (3.15), for constant volume (3.18). The asymptotic representation of h is

$$h(x,t) \sim \frac{3}{4}\left\{\frac{a^2 - x^2}{a^3} + \hat{M}[2(a^2 + x^2)\ln(2a) - \tfrac{4}{3}(a^2 - x^2) - (a-x)^2 \ln(a-x) - (a+x)^2 \ln(a+x)]\right\}, \tag{7.2p}$$

$$h(r,t) \sim \frac{2}{\pi}\frac{a^2 - r^2}{a^4} + \tfrac{3}{8}\hat{M}\left[\sum_{n=1}^{\infty}\left(\frac{a}{n}\right)^2\left\{1 - \left(\frac{r}{a}\right)^{2n}\right\} + (a^2 - r^2)\left\{\ln\left(\frac{a^2 - r^2}{a^2}\right) - \frac{3}{2}\right\}\right]. \tag{7.2a}$$

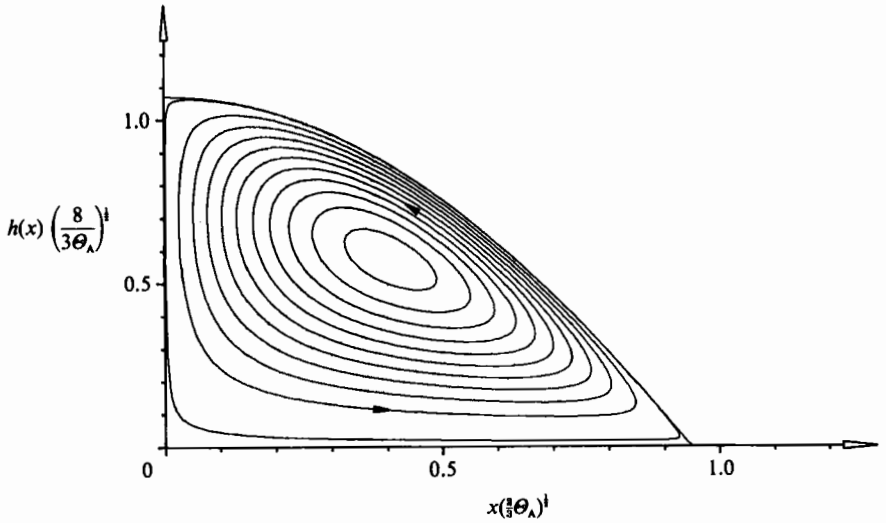

FIGURE 5. Non-isothermal spreading: steady drop shapes and streamlines for $\hat{M} = 0.2$, $G = 0$. The horizontal and vertical axes are rescaled using units appropriate to the steady drop under isothermal conditions.

We substitute (7.2) into the contact-angle conditions (3.17) and (3.19) to obtain

$$a_t^{1/m} + \Theta_A = -h_x(a,t) \sim \frac{3}{2a^2}(1 - \tfrac{1}{3}a^3\hat{M}), \tag{7.3p}$$

$$a_t^{1/m} + \Theta_A = -h_r(a,t) \sim \frac{4}{\pi a^3}\left(1 - \frac{3\pi}{32}a^4\hat{M}\right). \tag{7.3a}$$

Equations (7.3) are approximations of differential equations for $|\hat{M}| \ll 1$ with $a = a(t)$ subject to the initial conditions $a(0) = 1$.

Case 1: $\Theta_A > 0$, $G = 0$

The drop spreads to an equilibrium configuration with $a = a_\infty$ and the fluid flow approaches a steady state. From (7.3) it follows for small $|\hat{M}|$ that

$$a_\infty \sim a_\infty^0[1 - \tfrac{1}{4}\hat{M}a_\infty^0/\Theta_A] \tag{7.4p}$$

and

$$a_\infty \sim a_\infty^0[1 - \tfrac{1}{8}\hat{M}a_\infty^0/\Theta_A], \tag{7.4a}$$

where a_∞^0 is given by (6.3). By comparison with (6.4) it is seen that thermocapillarity on a heated plate acts oppositely to gravity.

The drop on a heated plate ($\hat{M} > 0$) exhibits a circulation driven by thermocapillarity as shown in figure 5. The higher surface tension at the drop summit and a lower surface tension at the edges are responsible for the liquid/gas interface being 'pulled' towards the drop summit. The flow is inward toward the centre where it turns around. This turning is driven by a pressure gradient in which there is a higher pressure at the centre and this deforms the drop; the interface steepens near the centre and flattens near the edge. This effect is similar to the deformation of the

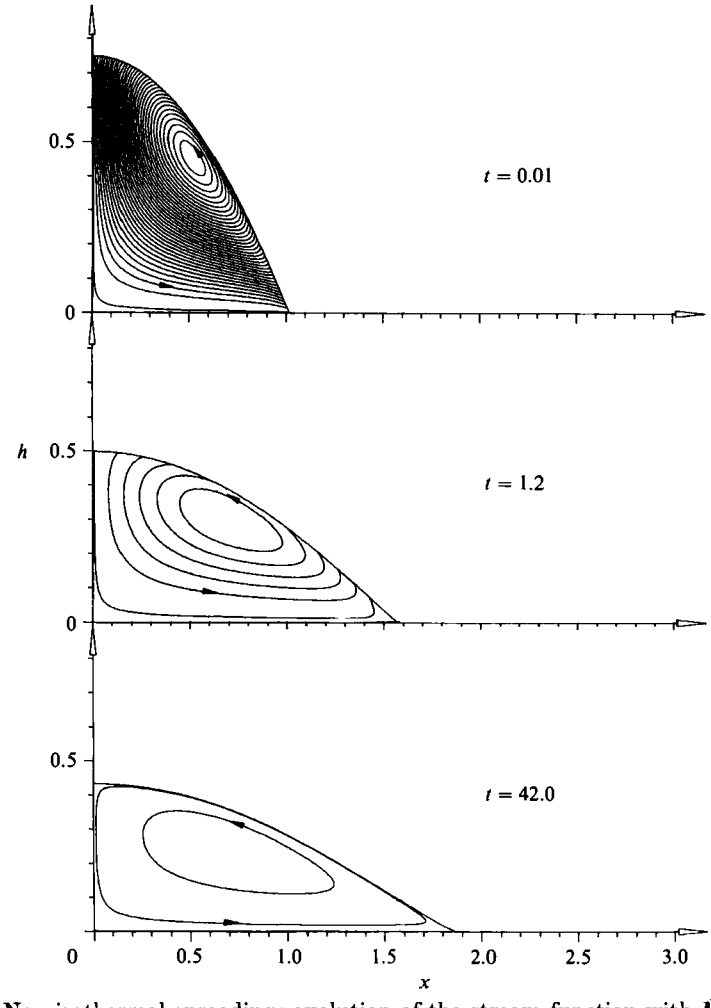

FIGURE 6. Non-isothermal spreading: evolution of the stream function with $\hat{M} = 0.2$, $\Theta_A = 0.25$ and $G = 0$. Instantaneous streamlines are given in steps $\Delta\psi = 0.01$.

surface in a slot caused by a recirculating thermocapillary flow as explained by Sen & Davis (1982). By conservation of mass, the edge is at a position $a_\infty < a_\infty^0$ as shown in (7.4p).

A comparison of the transient behaviour for $\hat{M} = 0$ and $\hat{M} > 0$ shows that the heating slows the spreading and limits the final drop size. The evolution to the final shape involves the spreading flow down the interface as shown in figure 3 and a counterflow up the interface driven by thermocapillarity. The result is the complex flow field shown in figure 6.

Equations (7.1)–(7.4) also hold for the case of a cooled plate, $\hat{M} < 0$. In such a situation the direction of the thermocapillary flow is reversed, resulting in a flatter drop with extended edges $a_\infty > a_\infty^0$ as given in (7.4). The thermocapillary-driven flow pulls liquid outward along the liquid/gas interface as shown in figure 7. Here the thermally driven flow aids the pure-spreading flow, shown in figure 3.

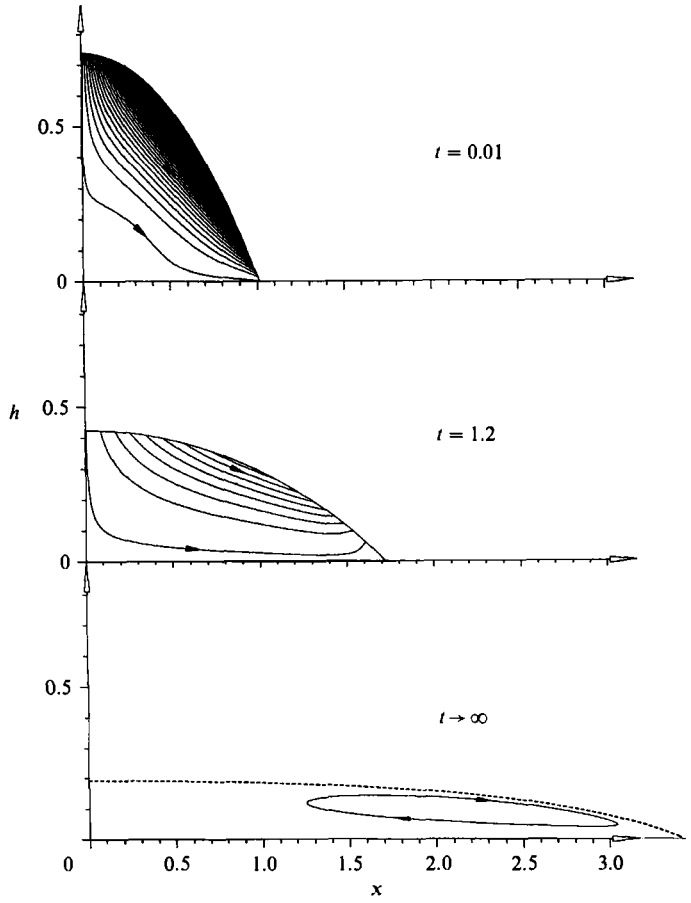

FIGURE 7. Non-isothermal spreading: evolution of velocity fields with $M = -0.1$, $\Theta_A = 0.25$ and $G = 0$. Given are instantaneous streamlines in steps $\Delta\psi = 0.01$. The dashed (solid) curve is obtained from equation (4.8p) (equation (7.3p)).

Case 2: $\Theta_A = 0$, $G = 0$

In the absence of thermocapillarity, a drop with $\Theta_A = 0$ will spread to infinity as shown by (7.3) with $\hat{M} = 0$. When $\Theta_A = 0$ and $\hat{M}$ is positive and small, it may be that $h_x(a_\infty, \infty) = 0$ or $h_r(a_\infty, \infty) = 0$ for $a_\infty < \infty$. Equations (7.3) are not necessarily reliable here since if $\hat{M}$ is small, a_∞ is large and the conditions $a^3\hat{M} \ll 1$ or $a^4 M \ll 1$ will fail. However, (7.1) or (4.8) will be accurate and we now address the final states attained.

Case 3: Final spreading, $G = 0$

The effect of general heating can be investigated by solving system (4.8) numerically. Figure 8 shows such results for $\theta_A = 0$ and $\theta_A = 0.50$. In figure 8(a), $\Theta_A = 0$, we show a curve for a_∞ versus $\hat{M}$. When $\hat{M} = 0$, $a \to a_\infty^0$ as $t \to \infty$. If the plate is cooled, $\hat{M} < 0$, the spreading occurs faster and $a_\infty = \infty$ as well. For any degree for heating, $\hat{M} > 0$, thermocapillary effects prevent spreading to infinity so that $a_\infty < \infty$. In this two-dimensional case, $\Theta_A = G = 0$, one can infer the exact form of the curve. In the Appendix we show that there is a constant k such that

$$a^3\hat{M} = k^3 \qquad (7.5p)$$

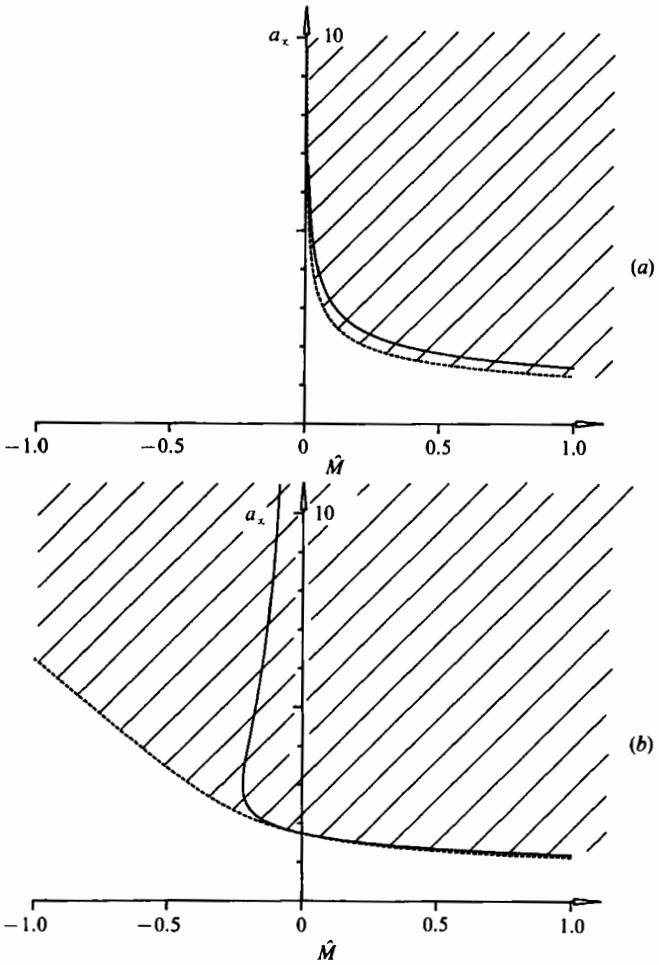

FIGURE 8. Final spreading: final drop widths a_∞ as functions of Marangoni number $\hat{M}$ for $G = 0$ and for two different advancing contact angles (*a*) $\Theta_A = 0$, and (*b*) $\Theta_A = 0.5$. The dashed (solid) curves are obtained from equation (4.8*p*) (equation (7.3*p*)).

for all $\hat{M}$. We obtain from our numerical solution that

$$k \approx 1.22. \tag{7.6p}$$

For this case, the small-$\hat{M}$ equations (7.3) are a reasonable approximation. If in these we set $a = a_\infty$ and $a_t = 0$, we find that

$$\hat{M} a_\infty^3 + 2\Theta_A a_\infty^2 - 3 = 0, \tag{7.7p}$$

$$\hat{M} a_\infty^4 + \tfrac{8}{3}\Theta_A a_\infty^3 - \frac{32}{3\pi} = 0. \tag{7.7a}$$

In the two-dimensional case for $\Theta_A = 0$, (7.7*p*) gives $k^3 = 3$ or $k \approx 1.44$.

In figure 8(*b*), $\Theta_A = 0.50$, we show a curve for a_∞ versus $\hat{M}$. Heating and cooling have their now expected effects. Various numerical cases have been investigated for Θ_A in the range [0.1, 0.5] and these give us approximate forms valid for $\hat{M} \to -\infty$.

$$a_\infty \sim -\frac{1.48}{\Theta_A^2}\hat{M}, \quad \hat{M} \to -\infty. \tag{7.8p}$$

When $\hat{M} > 0$, equations (7.3) for small $\hat{M}$ are applicable for all $\hat{M}$ as shown in figure 8(*b*). For $\theta_A \ll \hat{M}$,

$$a_\infty^3 \hat{M} \sim k_p \tag{7.9p}$$

$$a_\infty^4 \hat{M} \sim k_a \tag{7.9a}$$

for some constants k_p and k_a.

8. Discussion and conclusion

We have considered the spreading of Newtonian-viscous-liquid drops on a heated or cooled horizontal plate. We used lubrication theory to reduce the governing equations to a set of evolution equations for the interface shape h and the contact-line position a as defined in figure 1. This system includes the effects of viscosity, surface tension, gravity, thermocapillarity and wetting characteristics and generalizes the approach of Greenspan (1978) to non-isothermal systems with gravity and with power-law forms for $\theta = F(U)$. Both two-dimensional and axisymmetric drops have been examined for small capillary numbers.

8.1 *Isothermal spreading*

When gravity acts downward toward the plate, static drops ($\Theta_A > 0$) are flattened at their centres and hence extend outward further than they would in a gravity-free environment.

When the drop spreads finitely far, the final approach is exponential. However, at earlier times or if the drop spreads to infinity ($\Theta_A = 0$), the drop spreading follows a power law. We have found that gravitational forces can be very important on the scaling law at long times when the drop is very flat, even though they are negligible at earlier times when the drop is thicker. This prediction is in accord with the observations of Cazabat & Cohen Stuart (1987). Table 1 shows, if one takes the mobility exponent $m = 3$ so that $(\theta - \theta_A) \propto U^{\frac{1}{3}}$, that there is excellent agreement between the present theory and the existing isothermal experiments, a result that gives validation to both the $m = 3$ model and the uniform theory used. This uniform theory supposes that all local (molecular) physics at the contact line is incorporated into the function F of $\theta = F(U)$.

The approach used here could also be used to study spreading drops on the underside of the plate. One sets $G < 0$ and then examines the competition between viscous spreading and the tendency for pendant-drop formation. Yiantsios & Higgins (1989) study Rayleigh–Taylor instabilities of continuous film using (4.8) with $\beta = B = 0$, $C = 1$.

8.2. *Non-isothermal spreading*

In isothermal spreading capillary effects, which act along the whole liquid/gas interface, compete with the effects of wetting at the contact line. The influence of the heat transport is to create thermocapillary forces on the interface that enter the competition as well. They substantially retard (augment) the spreading when the plate is heated (cooled). They further create interfacial deformations; in the model posed the shape and slope are regular but the curvature is infinite at the contact line. Since the effect of thermocapillary is distributed along the whole interface, this locally integrable singularity should not be an important factor.

The general conclusion is that heating (cooling) the plate retards (augments) spreading. When $\Theta_A = 0$, the isothermal drop will spread to infinity. If the plate is heated, and $\Theta_A = 0$ still, then the drop will spread only finitely far no matter how

weakly the plate is heated. If $\Theta_A > 0$, the isothermal drop will always spread finitely far. We have examined the final states and determined the precise behaviour as a function of heating/cooling and Θ_A. These results show the existence of a mechanism for the thermal control of spreading, one that is quite sensitive to thermal gradients.

There are a number of generalizations of the present work that would be interesting. A direct numerical simulation of the evolution equation could determine effects present when C is not small. Such results would overlap the model of Hocking (1977, 1981, 1983). Haley & Miksis (1991) have done such initial-value calculations in the isothermal case. More general thermal boundary conditions might be appropriate especially if one wishes to model more precisely the contact-line region. (Near the contact line the convective boundary layer in the gas, modelled by the heat-transfer coefficient, is thicker than the liquid film.) The heat transport in our model is conduction dominated. Thus, the thermocapillary circulation transports little heat, though this transport might become substantial if the heating were more intense. Convective effects might be incorporated into the evolution equation as well as variations with temperature of the viscosity. We have a uniformly heated plate so that the advancing contact angle Θ_A, a local value, is constant. If the plate had non-uniform temperature, then one might have to account for $\Theta_A = \Theta_A(T)$, or more generally, $\Theta = F(U, T)$.

The present work suggests experiments of several varieties. One class could involve qualitative questions such as augmentation or retardation of spreading by heat transfer. A second class could involve quantitative explorations into power laws for spreading, and interface shapes.

One phenomenon that the experiments might reveal is the presence of a type of thermocapillary instability in cases where the plate is heated. Consider such a drop that has spread to its finite equilibrium. If the thermocapillary-driven motion were absent and the layer had uniform thickness $h_0 = 1$, then one could analyse the instability of the state via (4.8) with $\beta = 0$ and, say, $\tau = C^{-1}t$. This has been done by Burelbach, Davis & Bankoff (1988) in their §9 if one sets $E = 0$, $K \gg 1$. In our notation for the two-dimensional case they would predict steady, cellular instabilities if both $\hat{M}/G > 1$ and $a_\infty > \frac{1}{2}\pi(\hat{M}-G)^{-1}$ hold. Such instabilities might lead to multicellular flows rather than the double cell seen above. Clearly, such conclusions about instability would be modified by the fact that $h_0 = h_0(x)$ for the drop, that there is motion within the drop, and that there are contact-line conditions that must hold. If such instabilities were present, then they would also be present before the drop reached its final state and so would affect the spreading rates. In sum, the full stability problem could be addressed using the evolutionary system derived here, and experimenters should be alerted to the potential presence of this more complex behaviour.

P.E. is pleased to acknowledge the support of the Kernforschungszentrum Karlsruhe in his visit to Northwestern University. S.H.D. gratefully acknowledges the support of the US Department of Energy, Division of Basic Energy Sciences, through Grant no. DEFG02-86ER13641.

Appendix. Integration of the two-dimensional quasi-static equation for $\Theta_A = 0$

Consider, for $G = 0$, equation (7.1p) and its associated side conditions:

$$h_{xx} + \tfrac{3}{2}\hat{M} \ln h = -s_1, \tag{A 1a}$$

$$h_x(0) = 0, \tag{A 1b}$$

$$h(a) = 0, \quad h_x(a) = 0, \tag{A 1c}$$

$$2\int_0^a h \, dx = 1. \tag{A 1d}$$

Multiply (A 1a) by h_x, integrate and use the given conditions to obtain

$$h_x^2 = 3Mh \ln \frac{h_m}{h}, \tag{A 2}$$

where $h(0) = h_m$ is at the moment unknown. Define

$$v = \left[\tfrac{1}{2} \ln \frac{h_m}{h}\right]^{\frac{1}{2}} \tag{A 3}$$

and transform (A 2) to the following:

$$e^{-v^2} dv = \pm \frac{1}{2}\left(\frac{3\hat{M}}{2h_m}\right)^{\frac{1}{2}} dx. \tag{A 4}$$

Now integrate (A 4) up to the contact line at $x = a$,

$$\int_v^\infty e^{-\xi^2} d\xi = \frac{1}{2}\left(\frac{3\hat{M}}{2h_m}\right)^{\frac{1}{2}} (a - x), \tag{A 5}$$

where we have chosen the positive root. Evaluate (A 5) at the apex: $x = 0$, $v = 0$ to obtain

$$h_m = \frac{3\hat{M}}{2\pi} a^2. \tag{A 6}$$

Now, substitute (A 6) into (A 4) and (A 5), and find from (A 5) that, for some function F,

$$F(v) = \frac{\pi^{\frac{1}{2}}}{2a}(a - x). \tag{A 7}$$

Solve for v and there is a function G, related to F^{-1}, that gives

$$h = \frac{3\hat{M}a^2}{2\pi} G\left[\frac{\pi^{\frac{1}{2}}}{2}(a - x)\right]. \tag{A 8}$$

We now apply to volume constraint (A 1d) to (A 8) and obtain that

$$\frac{3\hat{M}a^3}{\pi} \int_0^1 G\left[\frac{\pi^{\frac{1}{2}}}{2}(1 - X)\right] dX = 1, \tag{A 9}$$

where $X \equiv x/a$. Since the integral is independent of a, there exists a constant k such that

$$a^3\hat{M} = k^3 \tag{A 10}$$

for any $\hat{M} > 0$.

REFERENCES

BURELBACH, J. P., DAVIS, S. H. & BANKOFF, S. G. 1988 Nonlinear stability of evaporating/condensing liquid films. *J. Fluid Mech.* **195**, 463.

CAZABAT, A. M. & COHEN STUART, M. A. 1986 Dynamics of wetting: effects of surface roughness. *J. Phys. Chem.* **90**, 5845.

CHEN, J.-D. 1988 Experiments on a spreading drop and its contact angle on a solid. *J. Colloid Interface Sci.* **122**, 60.

DAVIS, S. H. 1980 Moving contact lines and rivulet instabilities. Part 1. The static rivulet. *J. Fluid Mech.* **98**, 225.

DAVIS, S. H. 1983 Contact-line problems in fluid mechanics. *Trans. ASME* E: *J. Appl. Mech.* **50**, 977.

DUSSAN V., E. B. 1976 The moving contact line: the slip boundary condition. *J. Fluid Mech.* **77**, 665.

DUSSAN V., E. B. 1979 On the spreading of liquids on solid surfaces: static and dynamic contact lines. *Ann. Rev. Fluid Mech.* **11**, 371.

DUSSAN V., E. B. 1987 On the ability of drops to stick to surfaces of solids. Part 3. The influences of the motion of the surrounding fluid on dislodging drops. *J. Fluid Mech.* **174**, 81.

DUSSAN V., E. B. & DAVIS, S. H. 1974 On the motion of a fluid–fluid interface along a solid surface. *J. Fluid Mech.* **65**, 71.

GENNES, P. G. DE 1985 Wetting: statics and dynamics. *Rev. Mod. Phys.* **57**, 827.

GREENSPAN, H. P. 1978 On the motion of a small viscous droplet that wets a surface. *J. Fluid Mech.* **84**, 125.

HALEY, P. J. & MIKSIS, M. J. 1991 The effects of the contact line on droplet spreading. *J. Fluid Mech.* **223**, 57.

HOCKING, L. M. 1977 A moving fluid interface. Part 2. The removal of the force singularity by a slip flow. *J. Fluid Mech.* **79**, 209.

HOCKING, L. M. 1981 Sliding and spreading of thin two-dimensional drops. *Q. J. Mech. Appl. Maths.* **34**, 37.

HOCKING, L. M. 1983 The spreading of thin drops by gravity and capillarity. *Q. J. Mech. Appl. Maths.* **36**, 55.

HOCKING, L. M. & RIVERS, A. D. 1982 The spreading of a drop by capillary action. *J. Fluid Mech.* **121**, 425.

HOFFMAN, R. L. 1975 A study of the advancing interface. I. Interface shape in liquid–gas systems, *J. Colloid Interface Sci.* **50**, 228.

LOPEZ, J., MILLER, C. A. & RUCKENSTEIN, E. 1976 Spreading kinetics of liquid drops on solids. *J. Colloid Interface Sci.* **56**, 460.

NGAN, C. G. & DUSSAN V., E. B. 1989 On the dynamics of liquid spreading on solid surfaces. *J. Fluid Mech.* **209**, 191.

ROSENBLAT, S. & DAVIS, S. H. 1985 How do liquid drops spread on solids? In *Frontiers in Fluid Mechanics* (ed. S. H. Davis & J. L. Lumley), p. 171. Springer.

SCHWARTZ, A. M. & TEJEDA, S. B. 1972 Studies of dynamic contact angles on solids. *J. Colloid Interface Sci.* **38**, 359.

SEN, A. K. & DAVIS, S. H. 1982 Steady thermocapillary flows in two-dimensional slots. *J. Fluid Mech.* **121**, 163.

STAROV, V. M. 1983 Spreading of droplets of nonvolatile liquids over a flat surface. *Colloid J. USSR* (Eng. transl.) **45**, 1009.

TANNER, L. H. 1979 The spreading of silicone oil on horizontal surfaces. *J. Phys.* D: *Appl. Phys.* **12**, 1473.

YIANTSIOS, S. G. & HIGGINS, B. G. 1989 Rayleigh–Taylor instability in thin viscous films. *Phys. Fluids* A **1**, 1484.